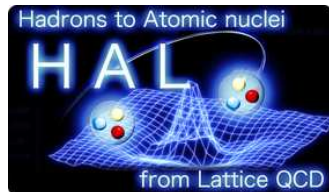


ΛN and ΞN Interactions Studied with Lattice QCD

H. Nemura^a for HAL QCD Collaboration

Department of Physics, Tohoku University, Sendai, 980-8578, Japan



Abstract. We present our recent studies of Lambda-Nucleon (ΛN) as well as Cascade-Nucleon (ΞN) interactions by using lattice QCD. The equal-time Bethe-Salpeter (BS) amplitude of the lowest energy scattering state of baryon number $B = 2$ system (proton- Λ and proton- Ξ^0) is calculated from lattice QCD. For the calculation of the ΛN potential, two different types of gauge configurations are employed: (i) 2+1 flavor full QCD configurations generated by the PACS-CS collaboration at $\beta = 1.9$ ($a = 0.0907(13)$ fm) on a $32^3 \times 64$ lattice, whose spatial volume is $(2.90 \text{ fm})^3$. (ii) Quenched QCD configurations at $\beta = 5.7$ ($a = 0.1416(9)$ fm) on a $32^3 \times 48$ lattice, whose spatial volume is $(4.5 \text{ fm})^3$. The spin-singlet central potential is calculated from the BS wave function for the spin $J = 0$ state, whereas the spin-triplet central potential as well as the tensor potential are deduced simultaneously from the BS wave function for the spin $J = 1$ state by dividing it into the S -wave and the D -wave components. For the calculation of the ΞN potential, we employ quenched QCD configurations, at $\beta = 5.7$ ($a = 0.1416(9)$ fm) on a $32^3 \times 32$ lattice, whose spatial volume is $(4.5 \text{ fm})^3$. The effective central potential in the spin triplet channel as well as the central potential in the spin singlet channel are calculated for the ΞN . The scattering lengths are obtained from the asymptotic behavior of the BS wave function by using the Lüscher's formula.

1 Introduction

Study of hyperon-nucleon (YN) and hyperon-hyperon (YY) interactions is one of the keys to explore strange nuclear systems such as hypernuclei and also hyperonic matter inside neutron stars. Hyperons (or strange quarks) would play a characteristic role in normal nuclear systems as “impurities” [1]. A number of spectroscopic studies of the Λ and Σ hypernuclei have been performed experimentally and theoretically; They lead a qualitative conclusion that the Σ -nucleus interaction is repulsive [2,3] whereas the Λ -nucleus interaction is attractive and the strength of Λ potential in nuclear systems is about 2/3 of the strength of the normal nuclear potential. Moreover, recent systematic study (e.g., Ref. [4]) for light (s -shell) Λ hypernuclei (${}^3_\Lambda\text{H}$, ${}^4_\Lambda\text{H}$, ${}^4_\Lambda\text{He}$ and ${}^5_\Lambda\text{He}$) suggests that the ΛN interaction in the 1S_0 channel is more attractive than that in the 3S_1 channel. These results is useful to study the composition of hyperonic matter inside the neutron stars [5]: the Λ particle instead of Σ^- would be the first strange baryon to appear in the core of the neutron stars. The ΞN interaction is also interesting and important, in order to explore the existence of Ξ hypernuclei and the dense hyperonic matter in neutron stars. Despite their importance, however, YN and YY inter-

actions have still large uncertainties because direct YN and YY scattering experiments are either difficult or impossible due to the short life-time of hyperons. Consequently, phenomenological YN and YY interaction models are not well constrained from experimental data even under some theoretical guides [6–11].

Under these circumstances, it should be desirable theoretically to understand the YN and YY interaction (or, in more general, baryon-baryon interaction) based on the dynamics of quarks and gluons as fundamental degrees of freedom. If one can perform such an appropriate deduction along the theory of quantum chromodynamics (QCD), they should have a reliable prediction regarding the YN and YY potentials.

The lattice QCD would be a valuable theoretical tool to perform a first-principle calculation of baryon-baryon interactions. Previously, scattering parameters based on the Lüscher's formula have been reported for the NN system [12,13] and for the YN system [14,15]. Recently, a new approach to the NN interaction from the lattice QCD has been proposed [16]. In this approach, the NN potential can be directly obtained from lattice QCD through the Bethe-Salpeter (BS) amplitude and the observables such as the phase shift and the binding energy can be calculated by using the resultant potential. The purpose of this report is

^a e-mail: nemura@nucl.phys.tohoku.ac.jp

to show the recent results for the YN potentials calculated from lattice QCD.

See Refs. [17–26] for the recent developments in various aspects along the line of this approach.

2 Formulation

The basic formulation has already been given in Refs. [16, 17, 20, 21]. (See also Refs. [27, 28].) and a recent comprehensive accounts for the lattice NN potential is found in Ref. [18]. We start from an effective Schrödinger equation for the equal-time BS wave function of two-baryon system (B_1B_2):

$$(\nabla^2 + k^2) \phi(\mathbf{r}) = 2\mu \int d^3r' U(\mathbf{r}, \mathbf{r}') \phi(\mathbf{r}'). \quad (1)$$

Here k^2 and $\mu = m_{B_1}m_{B_2}/(m_{B_1} + m_{B_2})$ are the square of asymptotic momentum in the center-of-mass frame and the reduced mass of the (B_1B_2) system, respectively. The total energy is given by

$$W = \sqrt{m_{B_1}^2 + k^2} + \sqrt{m_{B_2}^2 + k^2}. \quad (2)$$

We consider the low-energy scattering state so that the non-local potential can be rewritten by derivative expansion [29],

$$U(\mathbf{r}, \mathbf{r}') = V_{B_1B_2}(\mathbf{r}, \nabla) \delta(\mathbf{r} - \mathbf{r}'). \quad (3)$$

The general expression of the YN potentials ($V_{NA}, V_{N\Xi}$) are known to be [30]

$$\begin{aligned} V_{NY} &= V_0(r) + V_\sigma(r)(\sigma_N \cdot \sigma_Y) \\ &+ V_\tau(r)(\tau_N \cdot \tau_Y) + V_{\sigma\tau}(r)(\sigma_N \cdot \sigma_Y)(\tau_N \cdot \tau_Y) \\ &+ V_T(r)S_{12} + V_{T\tau}(r)S_{12}(\tau_N \cdot \tau_Y) \\ &+ V_{LS}(r)(\mathbf{L} \cdot \mathbf{S}_+) + V_{LS\tau}(r)(\mathbf{L} \cdot \mathbf{S}_+)(\tau_N \cdot \tau_Y) \\ &+ V_{ALS}(r)(\mathbf{L} \cdot \mathbf{S}_-) + V_{ALS\tau}(r)(\mathbf{L} \cdot \mathbf{S}_-)(\tau_N \cdot \tau_Y) \\ &+ O(\nabla^2). \end{aligned} \quad (4)$$

Here $S_{12} = 3(\sigma_N \cdot \mathbf{n})(\sigma_Y \cdot \mathbf{n}) - \sigma_N \cdot \sigma_Y$ is the tensor operator with $\mathbf{n} = \mathbf{r}/|\mathbf{r}|$, $\mathbf{S}_\pm = (\sigma_N \pm \sigma_Y)/2$ are symmetric (+) and antisymmetric (−) spin operators, $\mathbf{L} = -i\mathbf{r} \times \nabla$ is the orbital angular momentum operator, and τ_N (τ_Ξ) is isospin operator for $N = (p, n)^T$ ($\Xi = (\Xi^0, \Xi^-)^T$). Note that $\tau_\Lambda = 0$ due to the isospin-singlet nature of the Λ . The antisymmetric spin-orbit forces appear when the two baryons are not identical. $V_{0,\sigma,\tau,\sigma\tau,T,T\tau}$ are the leading order (LO) potentials while $V_{LS,LS\tau,ALS,ALS\tau}$ are the next-to-leading-order (NLO) potentials in the velocity expansion. For the present work of the ΞN interaction, since we focus on the isospin triplet ($I = 1$) channel a particular combination of the potential terms with $(\tau_N \cdot \tau_\Xi) = 1$ is taken into account,

$$V_{N\Xi}^{(I=1)} = (V_0 + V_\tau) + (V_\sigma + V_{\sigma\tau})(\sigma_N \cdot \sigma_Y) + \dots \quad (5)$$

For the sake of simplicity we rewrite them in what follows for the ΞN ($I = 1$) potential

$$(V_0 + V_\tau) \rightarrow V_0, \quad (V_\sigma + V_{\sigma\tau}) \rightarrow V_\sigma, \quad \dots \quad (6)$$

The LO potentials have been calculated along the line as follows. For the spin singlet state, we consider the central potential,

$$V_C(r; J = 0) = V_0(r) - 3V_\sigma(r) = \frac{(\nabla^2 + k^2)\phi(r)}{2\mu\phi(r)}. \quad (7)$$

For the spin triplet state, on the other hand, the wave function $\phi(\mathbf{r}; J = 1)$ comprises the S - and the D -wave components because of the tensor force. These partial waves can be extracted from the $\phi_{\alpha\beta}(\mathbf{r}; J = 1)$ such that

$$\begin{aligned} \phi_{\alpha\beta}(\mathbf{r}; {}^3S_1) &= \\ \mathcal{P}\phi_{\alpha\beta}(\mathbf{r}; J = 1) &\equiv \frac{1}{24} \sum_{\mathcal{R} \in O} \mathcal{R}\phi_{\alpha\beta}(\mathbf{r}; J = 1), \end{aligned} \quad (8)$$

$$\begin{aligned} \phi_{\alpha\beta}(\mathbf{r}; {}^3D_1) &= \\ \mathcal{Q}\phi_{\alpha\beta}(\mathbf{r}; J = 1) &\equiv (1 - \mathcal{P})\phi_{\alpha\beta}(\mathbf{r}; J = 1). \end{aligned} \quad (9)$$

Therefore, the effective Schrödinger equation with the LO potentials becomes:

$$\begin{aligned} \begin{Bmatrix} \mathcal{P} \\ \mathcal{Q} \end{Bmatrix} \times \{V_C(r; J = 1) + V_T(r)S_{12}\} \phi(\mathbf{r}) \\ = \begin{Bmatrix} \mathcal{P} \\ \mathcal{Q} \end{Bmatrix} \times \left(\frac{\nabla^2 + k^2}{2\mu} \right) \phi(\mathbf{r}), \end{aligned} \quad (10)$$

with

$$V_C(r; J = 1) = V_0(r) + V_\sigma(r). \quad (11)$$

The r dependence of the central and the tensor potentials, $V_C(r; J = 0)$, $V_C(r; J = 1)$ and $V_T(r)$, are determined once we obtain the wave function, the asymptotic momentum and the reduced mass in lattice QCD.

In order to obtain the $\phi_{\alpha\beta}(\mathbf{r}; J)$, we firstly calculate the four-point correlator from the lattice QCD

$$\begin{aligned} F_{\alpha\beta}^{(J,M)}(\mathbf{r}, t - t_0) &= \\ \sum_{\mathbf{X}} \left\langle 0 \left| B_{1,\alpha}(\mathbf{X} + \mathbf{r}, t) B_{2,\beta}(\mathbf{X}, t) \overline{\mathcal{J}_{B_1B_2}^{(J,M)}(t_0)} \right| 0 \right\rangle, \end{aligned} \quad (12)$$

where the summation over \mathbf{X} is to select the state with zero total momentum. The $B_{1,\alpha}(x)$ and $B_{2,\beta}(y)$ denote the interpolating fields of the baryons such as

$$p_\alpha(x) = \varepsilon_{abc} (u_a(x) C \gamma_5 d_b(x)) u_{c\alpha}(x), \quad (13)$$

$$\begin{aligned} \Lambda_\beta(y) &= \varepsilon_{abc} \left\{ (d_a(y) C \gamma_5 s_b(y)) u_{c\beta}(y) \right. \\ &\quad \left. + (s_a(y) C \gamma_5 u_b(y)) d_{c\beta}(y) \right. \\ &\quad \left. - 2(u_a(y) C \gamma_5 d_b(y)) s_{c\beta}(y) \right\}, \end{aligned} \quad (14)$$

$$\Xi_\beta^0(y) = \varepsilon_{abc} (u_a(y) C \gamma_5 s_b(y)) s_{c\beta}(y). \quad (15)$$

$\overline{\mathcal{J}_{B_1B_2}^{(J,M)}(t_0)} = \sum_{\alpha'\beta'} P_{\alpha'\beta'}^{(J,M)} \overline{B_{1,\alpha'}(t_0) B_{2,\beta'}(t_0)}$ is the source to create a B_1B_2 state with performing the spin projection for the total angular momentum J, M . The baryon sources $\overline{B}_{1,\alpha}, \overline{B}_{2,\beta}$ can be given by,

$$\overline{p}_\alpha = \varepsilon_{abc} (\overline{U}_a C \gamma_5 \overline{D}_b) \overline{U}_{c\alpha}, \quad (16)$$

Table 1. Hadron masses in the unit of MeV.

κ_{ud}	m_π	m_ρ	m_K	m_{K^*}	m_N	m_Λ	m_Σ	m_Ξ
$N_{Flavor} = 2 + 1$ QCD by PACS-CS with $\kappa_s = 0.13640$								
0.13700	699.4(4)	1108(3)	786.8(4)	1159(2)	1572(6)	1632(4)	1650(5)	1701(4)
0.13727	567.9(6)	1000(4)	723.7(7)	1081(3)	1396(6)	1491(4)	1519(5)	1599(4)
0.13754	413.6(6)	902(3)	636.6(4)	1026(3)	1221(7)	1349(4)	1406(8)	1505(4)
0.13770	301(3)	845(10)	592(1)	980(6)	1079(12)	1248(15)	1308(13)	1432(7)
quenched QCD with $\beta = 5.7$, $\kappa_s = 0.1643$								
0.1665	511.8(5)	862(3)	605.8(5)	898(1)	1297(6)	1344(6)	1375(5)	1416(3)
0.1670	463.6(6)	842(4)	586.3(5)	895(2)	1250(9)	1314(9)	1351(6)	1404(4)
0.1675	407(1)	820(3)	564.9(5)	886(3)	1205(13)	1269(9)	1326(9)	1383(5)
Exp.	135	770	494	892	940	1116	1190	1320

$$\bar{\Lambda}_\beta = \varepsilon_{abc} \left\{ (\bar{D}_a C \gamma_5 \bar{S}_b) \bar{U}_{c\beta} + (\bar{S}_a C \gamma_5 \bar{U}_b) \bar{D}_{c\beta} - 2(\bar{U}_a C \gamma_5 \bar{D}_b) \bar{S}_{c\beta} \right\}, \quad (17)$$

$$\bar{\Xi}_\beta^0 = \varepsilon_{abc} (\bar{U}_a C \gamma_5 \bar{S}_b) \bar{S}_{c\beta}, \quad (18)$$

with

$$Q = \sum_{\mathbf{x}} q(t, \mathbf{x}) f(\mathbf{x}), \quad (Q, q) = (U, u), (D, d), (S, s). \quad (19)$$

The wall source ($f(\mathbf{x}) = 1$) is employed to calculate the lowest scattering state of the system.

In the Monte Carlo calculations, noise reductions are made for the four-point correlator (12) obtained from lattice QCD in order to restore (i) the rotational (cubic group) symmetry, (ii) the spatial reflection symmetry, (iii) the charge conjugation and time-reversal symmetry.

The desirable wave function $\phi_{\alpha\beta}(\mathbf{r}; J)$ is obtained from the projected four-point correlator at large $t - t_0$:

$$\begin{aligned} F_{\alpha\beta}^{(J,M)}(\mathbf{r}, t - t_0) &= \sum_n A_n \sum_{\mathbf{X}} \langle 0 | B_{1,\alpha}(\mathbf{X} + \mathbf{r}, t) B_{2,\beta}(\mathbf{X}, t) | E_n \rangle e^{-E_n(t-t_0)} \\ &\approx A_0 \phi_{\alpha\beta}(\mathbf{r}; J, M) e^{-E_0(t-t_0)} \quad (t - t_0 \rightarrow \text{large}). \end{aligned} \quad (20)$$

Here E_n ($|E_n\rangle$) is the eigen-energy (eigen-state) of the six-quark system with the particular quantum number (i.e., J^π , M , strangeness S and isospin I), and

$$A_n = \sum_{\alpha'\beta'} P_{\alpha'\beta'}^{(JM)} \langle E_n | \bar{B}_{2,\beta'} \bar{B}_{1,\alpha'} | 0 \rangle. \quad (21)$$

3 Lattice setup

3.1 $N_{Flavor} = 2 + 1$ full QCD

The ΛN potentials have been calculated by using the 2+1 flavor full QCD gauge configurations generated by PACS-CS collaboration [31] with the RG-improved Iwasaki gauge action and the nonperturbatively $O(a)$ -improved Wilson quark action at $\beta = 1.9$ on a $32^3 \times 64$ lattice. The lattice spacing at the physical quark masses has

been estimated as $a = 0.0907(13)$ fm [31]. So far, we have employed four values of the hopping parameter for light quarks, $\kappa_{ud} = 0.13700, 0.13727, 0.13754, 0.13770$, while the one for the strange quark is fixed to $\kappa_s = 0.13640$. Several light hadron masses obtained in the present calculation are shown in Table 1. To calculate the BS wave function, the wall source is placed at the time-slice t_0 with the Coulomb gauge fixing, and the Dirichlet boundary condition is imposed in the temporal direction at the time-slice $t - t_0 = 32$. In order to improve the statistics, multiple sources at $t_0 = 8n$ with $n = 0, 1, 2, \dots, 8$ are employed on each gauge configuration. The results are obtained with $N_{\text{conf}} = 609, 481, 568, 422$ for $\kappa_{ud} = 0.13700, 0.13727, 0.13754, 0.13770$, respectively, where N_{conf} is the number of the gauge configurations.

3.2 Quenched calculation

In quenched QCD calculation we employ the plaquette gauge action and the Wilson quark action at $\beta = 5.7$ on a $32^3 \times 48$ ($32^3 \times 32$) lattice for the recent study of ΛN [22] (for the relatively earlier study of $p\Xi^0$ [20]). The periodic boundary condition is imposed for quarks in the spatial direction. The source is placed at t_0 with the Coulomb gauge fixing and the Dirichlet boundary condition is imposed in the temporal direction. The lattice spacing at the physical point is determined as $a = 0.1416(9)$ fm ($1/a = 1.393(9)$ GeV) from $m_\rho = 770$ MeV. The spatial lattice volume is about $(4.5\text{fm})^3$. The hopping parameter for the strange quark mass is given by $\kappa_s = 0.16432(6)$ from $m_K = 494$ MeV. Three values of the hopping parameter, $\kappa_{ud} = 0.1665, 0.1670, 0.1675$, are employed for the light quark mass when the ΛN potentials are calculated, while two values of the hopping parameter, $\kappa_{ud} = 0.1665, 0.1678$, are applied for the $p\Xi^0$ potentials. Table 1 also lists the light hadron masses calculated in quenched QCD. The results in quenched QCD are obtained with $N_{\text{conf}} \approx 1000$.

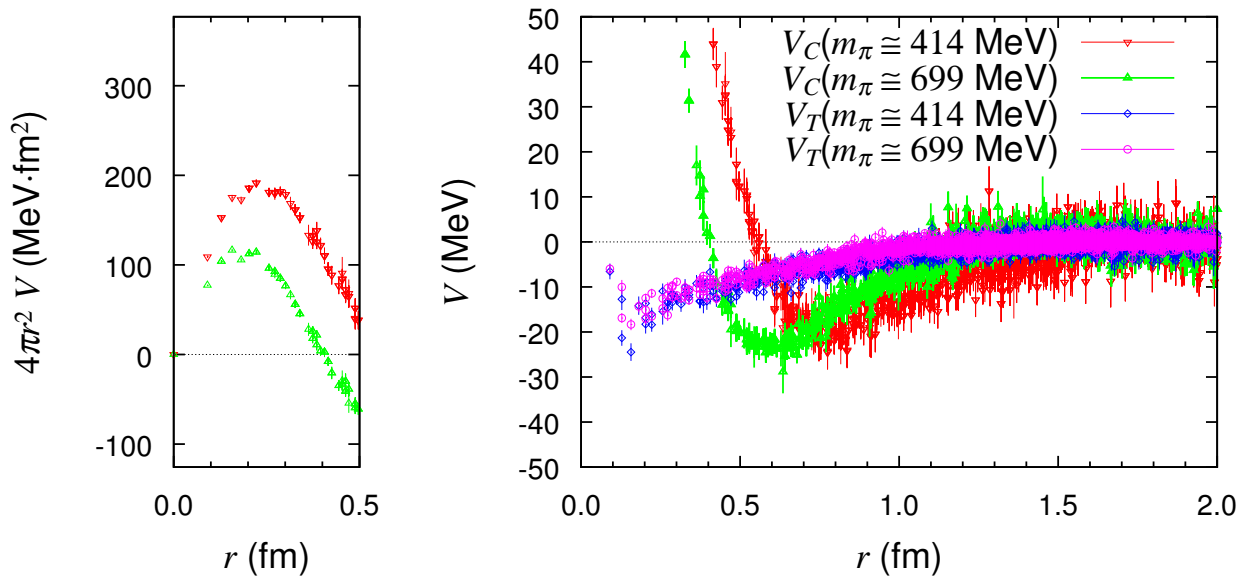


Fig. 1. The central and the tensor potentials in ${}^3S_1 - {}^3D_1$ channel in 2 + 1 flavor QCD as a function of r at $m_\pi \approx 414$ MeV (downward red triangle and blue diamond) and 699 MeV (upward green triangle and magenta circle). Figure taken from Ref. [24].

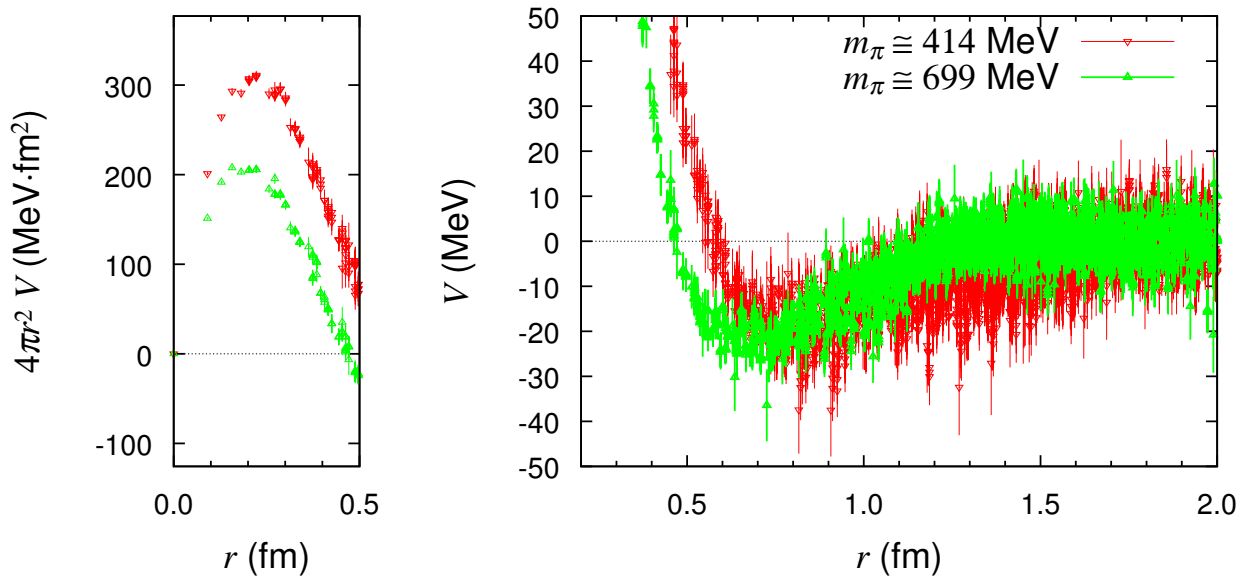


Fig. 2. The central potential in 1S_0 channel in 2 + 1 flavor QCD as a function of r at $m_\pi \approx 414$ MeV (downward red triangle) and 699 MeV (upward green triangle). Figure taken from Ref. [24].

4 Results

4.1 ΛN interaction

4.1.1 $N_{Flavor} = 2 + 1$ full QCD calculation

We first show the ΛN potential. Figures 1 and 2 taken from [24] show the ΛN potentials obtained from 2+1 flavor QCD calculation as a function of r . The central ($V_C(J = 1)$) and the tensor (V_T) potentials in the ${}^3S_1 - {}^3D_1$ channels are given in Fig. 1 while the central potential in the 1S_0 channel ($V_C(J = 0)$) is given in Fig. 2. We also show the

central potential multiplied by volume factor ($4\pi r^2 V_C(r)$) in the left panel in addition to the normal $V(r)$ given in the right panel, in order to compare the strength of the repulsive force between two quark masses. These figures contain results with $(m_\pi, m_K) \approx (699, 787)$ and $(414, 637)$ MeV, which are obtained at $t - t_0 = 13$ and 10, respectively. These time-slices are chosen so that the ground state saturation is achieved.

As can be seen in both figures, the attractive well of the central potential moves to outer region as the u, d quark mass decreases while the depth of these attractive pockets do not change so much. The present results show that

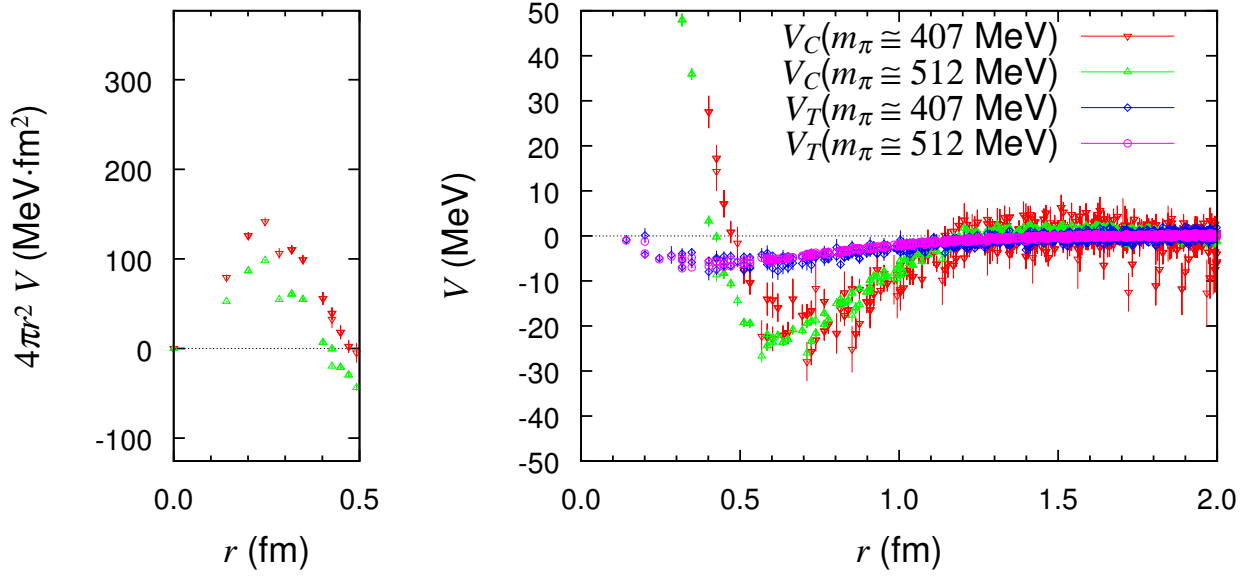


Fig. 3. The central and the tensor potentials in ${}^3S_1 - {}^3D_1$ channel of ΛN system in quenched QCD at $m_\pi \approx 407$ MeV (downward red triangle and blue diamond) and 512 MeV (upward green triangle and magenta circle). Figure taken from Ref. [24].

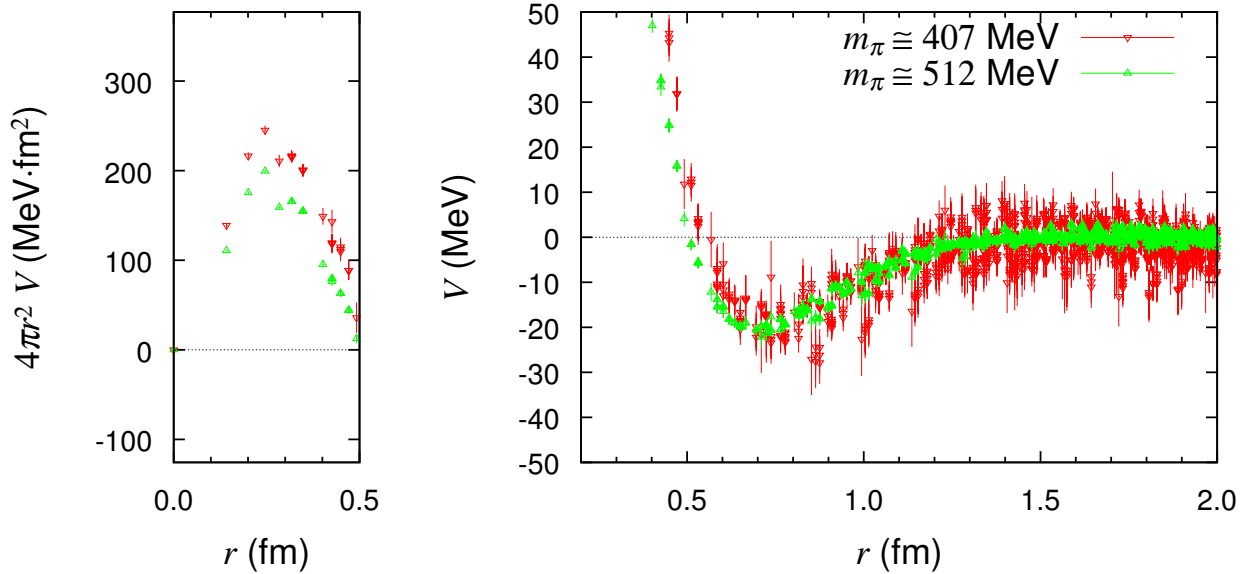


Fig. 4. The central potential in 1S_0 channel of ΛN system in quenched QCD at $m_\pi \approx 407$ MeV (downward red triangle) and 512 MeV (upward green triangle). Figure taken from Ref. [24].

the tensor force is weaker than the NN case [21], and the quark mass dependence of the tensor force seems to be small. Both of the repulsive and attractive parts increase in magnitude as the u, d quark mass decreases.

For $m_\pi \approx 699$ MeV, the central potentials reach $V_C \rightarrow 0$ at the radial distance $r \sim 1.3$ fm, which is smaller than the half of the physical lattice length ($aL/2 \approx 1.45$ fm). Therefore the Lüscher's formula can be applied to extract the scattering phase shift, which will be discussed in the latter section. For $m_\pi \approx 400$ MeV, on the other hand, the interaction range of the V_C , which is about 1.4 fm, almost reaches to the half of the lattice. Therefore we must be very

careful to extract the scattering phase shift at this or lighter quark masses from the Lüscher's formula, though no sign of the violation against the Lüscher's condition was observed within errors for the effective central potential even at $m_\pi \approx 300$ MeV. (See Fig. 1 in an earlier report [22].) Calculation on larger spatial volume will be needed to correctly extract the scattering phase shift at $m_\pi \approx 300$ MeV.

4.1.2 Quenched calculation

The ΛN potential is also calculated by quenched QCD. Figures 3 and 4 show the ΛN potentials obtained from

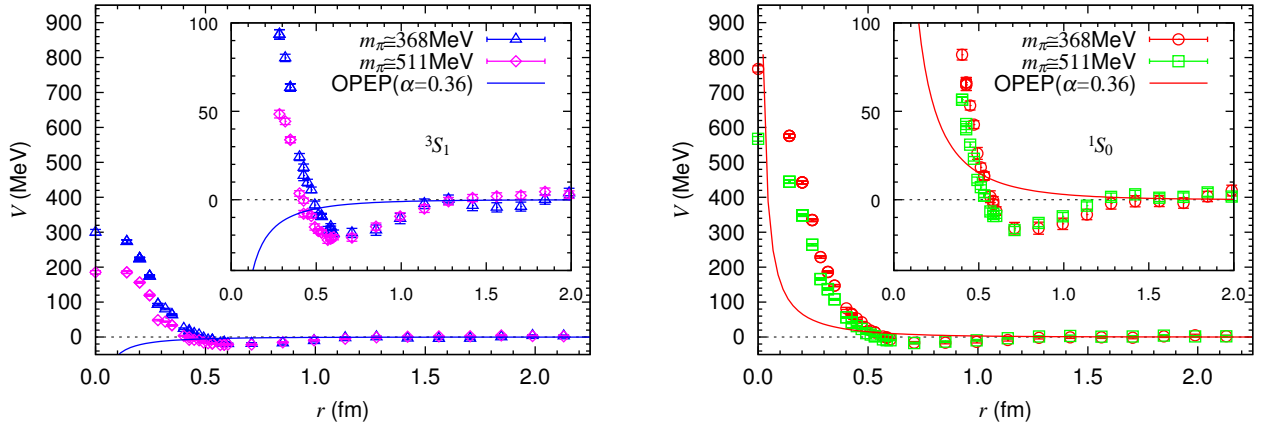


Fig. 5. Left: The effective central potential for $p\Xi^0$ in the 3S_1 channel at $m_\pi \simeq 368$ MeV (blue triangle) and $m_\pi \simeq 511$ MeV (magenta diamond). The central part of the OPEP ($F/(F+D) = 0.36$) is also given by solid line. Right: Same as the left figure, but in the 1S_0 channel at $m_\pi \simeq 368$ MeV (red circle) and $m_\pi \simeq 511$ MeV (green box). Figure taken from Ref. [20].

quenched QCD calculation. The central ($V_C(J=1)$) and the tensor (V_T) potentials for $J=1$ channel are given in the Fig. 3 while the central potential for $J=0$ channel ($V_C(J=0)$) is given in the Fig. 4. Comparing the strength of the repulsive cores between two quark masses, the central potential multiplied by volume factor ($4\pi r^2 V_C(r)$) is also shown in the left panel as well as the normal $V(r)$ in the right panel for each Figure. These figures contain results with $(m_\pi, m_K) \approx (512, 606)$ and $(407, 565)$ MeV, which are obtained at $t-t_0 = 7$. As can be seen in both figures, qualitative behavior of the potentials is similar to those of the full QCD potentials. Namely, the attractive well of the central potential moves to outer region as the u, d quark mass decreases while the depth of these attractive pockets do not change so much. The tensor force is weaker than the NN case, and the quark mass dependence of the tensor force seems to be small. Both of the repulsive and attractive parts increase in magnitude as the u, d quark mass decreases.

4.2 ΞN interaction

For ΞN interaction, we focus on the isovector ($I=1$) channel, which has no strong decay mode into other $B'_1 B'_2$ systems. (Note that, on the other hand, $N\Xi$ in the isoscalar ($I=0$) channel is above the $\Lambda\Lambda$ threshold.) As is also seen in Table 1, the baryon masses calculated from the lattice QCD are consistent with the experimentally observed ordering of the two-baryon threshold in the strangeness $S=-2$ sector; $E_{th}(\Lambda\Lambda) < E_{th}(N\Xi) < E_{th}(\Lambda\Sigma) < E_{th}(\Sigma\Sigma)$. This guarantees that the ΞN in the $I=1$ channel presented here is actually the lowest energy scattering state.

Figure 5 taken from Ref. [20] compares the (effective) central $p\Xi^0$ potential at $m_\pi \simeq 368$ MeV with that at $m_\pi \simeq 511$ MeV in the 3S_1 channel (left) and in the 1S_0 channel (right). At $m_\pi \simeq 368$ (511) MeV, the potentials are evaluated at $t-t_0 = 6$ (7). The height of the repulsive core increases as the ud quark mass decreases, while the significant difference is not seen in the medium to long distances

within the error bars. The solid lines in Fig.5 are the one pion exchange potential (OPEP),

$$V_C^\pi = -(1-2\alpha) \frac{g_{\pi NN}^2 (\tau_N \cdot \tau_\Xi)(\sigma_N \cdot \sigma_\Xi)}{4\pi \cdot 3} \left(\frac{m_\pi}{2m_N} \right)^2 \frac{e^{-m_\pi r}}{r}, \quad (22)$$

with $m_\pi \simeq 368$ MeV, $m_N \simeq 1167$ MeV and the empirical values, $\alpha \simeq 0.36$ [32] and $g_{\pi NN}^2/(4\pi) \simeq 14.0$ [33]. The pseudo-vector πNN coupling $f_{\pi NN}$ and the $\pi\Xi\Xi$ coupling $f_{\pi\Xi\Xi}$ are related as $f_{\pi\Xi\Xi} = -f_{\pi NN}(1-2\alpha)$ with the parameter $\alpha = F/(F+D)$ [6]. Also we define $g_{\pi NN} \equiv f_{\pi NN} \frac{m_\pi}{2m_N}$. Unlike the NN potential in the S -wave, the OPEP in the present case has opposite sign between the spin-singlet channel and the spin-triplet channel. Also, the absolute magnitude of OPEP is weak due to the factor $1-2\alpha$. From Fig.5, clear signature of OPEP at long distance ($r > 1.2$ fm) is hardly found within statistical errors. On the other hand, there is a clear departure from OPEP at medium distance ($0.6\text{fm} < r < 1.2\text{fm}$) in both 1S_0 and 3S_1 channels. These observations may indicate a mechanism of state-independent attraction such as the correlated two pion exchange.

5 Scattering length

The scattering parameters can be obtained from the asymptotic momentum k of the BS wave function according to Lüscher's formula [27,28], which is given by

$$k \cot \delta_0(k) = \frac{2}{\sqrt{\pi}L} Z_{00}(1; (kL/(2\pi))^2) = \frac{1}{a_0} + O(k^2), \quad (23)$$

with

$$Z_{00}(s; q^2) = \frac{1}{\sqrt{4\pi}} \sum_{\mathbf{n} \in \mathbb{Z}^3} (n^2 - q^2)^{-s} \quad \left(\text{Re } s > \frac{3}{2} \right), \quad (24)$$

where $Z_{00}(1; q^2)$ is obtained by the analytic continuation in s . The asymptotic momentum k on the finite lattice volume

is determined by fitting the asymptotic region of the BS wave function in terms of the Green's function

$$G(\mathbf{r}, k^2) = \frac{1}{L^3} \sum_{\mathbf{p} \in \Gamma} \frac{1}{p^2 - k^2} e^{i\mathbf{p}\cdot\mathbf{r}}, \quad (25)$$

$$\Gamma = \left\{ \mathbf{p}, \mathbf{p} = \mathbf{n} \frac{2\pi}{L}, \mathbf{n} \in \mathbf{Z}^3 \right\}, \quad (26)$$

which is the solution to the Helmholtz equation

$$(\nabla^2 + k^2)G(\mathbf{r}, k^2) = -\delta_L(\mathbf{r}), \quad (27)$$

with $\delta_L(\mathbf{r})$ being the periodic delta function [27,28]. Figure 6 (Figure 7) shows the scattering lengths for ΛN (ΞN ($I = 1$)) as a function of m_π^2 . Note that the sign of the S -wave scattering length a_0 defined in Eq. (23) becomes positive when the interaction is weakly attractive (i.e., there is no bound state.). What the Figures show at present is that both of ΛN and $p\Xi^0$ interactions are attractive on the whole. For the present results, the scattering lengths are almost constant for larger u, d quark mass region (corresponding to $m_\pi \gtrsim 500$ MeV). On the other hand, for lighter u, d quark mass (corresponding to $400 \text{ MeV} \lesssim m_\pi \lesssim 500 \text{ MeV}$), the present results seems to show that the scattering lengths increase as the u, d quark mass decreases. However, the actual quantities in the Fig. 6 are much smaller than the empirical values, $a_0^{\Lambda N}(^1S_0) \sim 1.5 - 2.5 \text{ fm}$, $a_0^{\Lambda N}(^3S_1) \sim 1.5 - 2.5 \text{ fm}$, estimated from the measurement of the ΛN total cross section and the theoretical studies of Λ -hypernuclei. And also diverse predictions on the $p\Xi^0$ scattering lengths from other approaches are summarized as follows: The chiral effective field theory [11] predicts $a_0(^1S_0) \sim -0.2 \text{ fm}$ and $a_0(^3S_1) \sim -0.02 \text{ fm}$. The phenomenological boson exchange model (e.g., SC97f) [6] gives $a_0(^1S_0) = -0.4 \text{ fm}$ and $a_0(^3S_1) = 0.030 \text{ fm}$. The quark cluster model (fss2) [8] gives $a_0(^1S_0) = -0.3 \text{ fm}$ and $a_0(^3S_1) = 0.2 \text{ fm}$, while QCD sum rules [10] gives $a_0(^1S_0) = 3.4 \pm 1.4 \text{ fm}$ and $a_0(^3S_1) = 6.0 \pm 1.4 \text{ fm}$. More extensive and systematic analysis with smaller lattice spacing, larger spatial volume and/or improved lattice action, etc., towards the physical quark mass point should be needed.

6 Summary

Recent studies of ΛN and ΞN interactions based on lattice QCD have been presented. The central and the tensor potentials are calculated from the BS wave function of the lowest energy scattering state for the ΛN system. The light-quark mass dependence of the central potentials shows that the interaction range becomes larger whereas the depth of the attractive well hardly changes as the u, d quark mass decreases. On the other hand, the tensor force of the ΛN interaction has relatively a weak light-quark mass dependence. It is also interesting to compare the present results with the NN potential found in Refs.[18,21]; The tensor force of the NN potential is significantly enhanced as the u, d quark mass decreases.

For the ΞN system, our lattice calculation shows that the $p\Xi^0$ interaction is attractive for both 1S_0 and 3S_1 states, whereas some phenomenological models predicts that the ΞN interaction for $I = 1$ channel is very weak or repulsive. A slight tendency that the 3S_1 interaction is relatively more attractive than that in the 1S_0 channels is found.

Finally, there are a few remarks before closing. Several related studies have been already carried out and/or started; (i) The study of the NN interaction is considerably important. See, for example, Refs. [18,21] for recent developments. (ii) In order to see how well the LO part in derivative expansion of the non-local potential $U(r, r')$ describes the interaction, the LO NN potential obtained at $E_{\text{c.m.}} \approx 45 \text{ MeV}$ have been compared with that at $E_{\text{c.m.}} \approx 0 \text{ MeV}$ [19,25]. The potentials are almost identical between these energies. It seems that the energy dependence of the NN potential is weak between these energies. (iii) Baryon-baryon potentials at the flavor $SU(3)$ limit have been calculated [23]. The flavor symmetry would be a good guide to understand the role of strangeness degree of freedom. The lattice QCD potential is the best tool to see the flavor symmetric world because it is a first-principle approach. (iv) $K + N$ (strangeness $S = +1$) channel potential is one of the interesting targets of this approach [26]. It is directly connected to searching for Θ^+ . (v) Three-nucleon force is an important puzzle to be clarified to make a nucleus comprising more than two nucleons from QCD. The calculation for the NNN system will be performed in the near future.

The full QCD calculations have been done by using PACS-CS computer under the "Interdisciplinary Computational Science Program" of Center for Computational Science, University of Tsukuba (No 09a-11). The quenched QCD calculations have been done by using Blue Gene/L computer under the "Large scale simulation program" at KEK (No. 09-23). Part of numerical analysis has been carried out with the help of special computer resource at Advanced Meson Science Laboratory of RIKEN Nishina Center. The author is supported by the Global COE Program for Young Researchers at Tohoku University (No. 22210005). This research was partly supported by the MEXT Grant-in-Aid, Scientific Research on Priority Areas (No. 20028013) and Scientific Research on Innovative Areas (Nos. 21105515, 20105003).

References

1. Reviewed in O. Hashimoto and H. Tamura, Prog. Part. Nucl. Phys. **57**, 564 (2006).
2. P. K. Saha *et al.*, Phys. Rev. C **70**, 044613 (2004) [arXiv:nucl-ex/0405031].
3. E. Friedman and A. Gal, Phys. Rept. **452**, 89 (2007) [arXiv:0705.3965 [nucl-th]].
4. H. Nemura, Y. Akaishi and Y. Suzuki, Phys. Rev. Lett. **89**, 142504 (2002) [arXiv:nucl-th/0203013].
5. See e.g. J. Schaffner-Bielich, Nucl. Phys. A **804**, 309 (2008) [arXiv:0801.3791 [astro-ph]].
6. T. A. Rijken, V. G. J. Stoks and Y. Yamamoto, Phys. Rev. C **59**, 21 (1999) [arXiv:nucl-th/9807082].

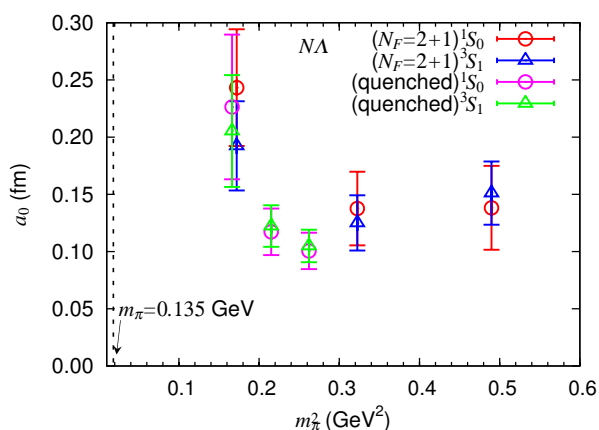


Fig. 6. Scattering lengths for the AN , as a function of m_π^2 . The sign of the scattering length is defined so that weakly attractive interaction corresponds positive value. Figure taken from Ref. [24].

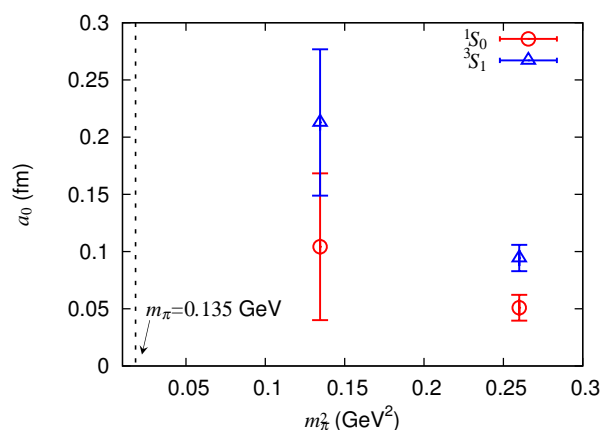


Fig. 7. Scattering lengths for the $\mathcal{E}N$ ($I = 1$), as a function of m_π^2 . The sign of the scattering length is defined so that weakly attractive interaction corresponds positive value. Figure taken from Refs. [20]($\mathcal{E}N$).

- T. A. Rijken and Y. Yamamoto, Phys. Rev. C **73**, 044008 (2006) [arXiv:nucl-th/0603042].
- T. A. Rijken and Y. Yamamoto, arXiv:nucl-th/0608074.
7. M. Oka, K. Shimizu and K. Yazaki, Prog. Theor. Phys. Suppl. **137**, 1 (2000).
 8. Y. Fujiwara, Y. Suzuki and C. Nakamoto, Prog. Part. Nucl. Phys. **58**, 439 (2007) [arXiv:nucl-th/0607013].
 9. I. Arisaka, K. Nakagawa, M. Wada and S. Shinmura, Prog. Theor. Phys. **113**, 1287 (2005).
 10. Y. Kondo and O. Morimatsu, Phys. Rev. C **69**, 055201 (2004).
 11. J. Haidenbauer, U. G. Meissner, A. Nogga and H. Polinder, Lect. Notes Phys. **724**, 113 (2007) [arXiv:nucl-th/0702015].
H. Polinder, J. Haidenbauer and U. G. Meissner, Phys. Lett. B **653**, 29 (2007) [arXiv:0705.3753 [nucl-th]].
H. Polinder, arXiv:0708.0773 [nucl-th].
 12. M. Fukugita, Y. Kuramashi, M. Okawa, H. Mino and A. Ukawa, Phys. Rev. D **52**, 3003 (1995) [arXiv:hep-lat/9501024].
 13. S. R. Beane, P. F. Bedaque, K. Orginos and M. J. Savage, Phys. Rev. Lett. **97**, 012001 (2006) [arXiv:hep-lat/0602010].
 14. S. Muroya, A. Nakamura and J. Nagata, Nucl. Phys. Proc. Suppl. **129**, 239 (2004).
 15. S. R. Beane *et al.* [NPLQCD Collab.], Nucl. Phys. A **794**, 62 (2007).
 16. N. Ishii, S. Aoki, T. Hatsuda, Phys. Rev. Lett. **99**, 022001 (2007).
 17. S. Aoki, T. Hatsuda and N. Ishii, Comput. Sci. Dis. **1**, 015009 (2008) [arXiv:0805.2462 [hep-ph]].
 18. S. Aoki, T. Hatsuda and N. Ishii, arXiv:0909.5585 [hep-lat].
 19. S. Aoki, J. Balog, T. Hatsuda, N. Ishii, K. Murano, H. Nemura and P. Weisz, arXiv:0812.0673 [hep-lat].
 20. H. Nemura, N. Ishii, S. Aoki and T. Hatsuda, Phys. Lett. B **673**, 136 (2009) [arXiv:0806.1094 [nucl-th]].
 21. N. Ishii, S. Aoki and T. Hatsuda, arXiv:0903.5497 [hep-lat].
 22. H. Nemura, N. Ishii, S. Aoki and T. Hatsuda [PACS-CS Collaboration], arXiv:0902.1251 [hep-lat].
 23. T. Inoue, [for HAL QCD Collaboration], arXiv:0911.2305 [hep-lat].
 24. H. Nemura, for HAL QCD and PACS-CS Collaboration, Proceedings of the XXVII International Symposium on Lattice Field Theory, (2009).
 25. K. Murano, for HAL QCD Collaboration, Proceedings of the XXVII International Symposium on Lattice Field Theory, (2009).
 26. Y. Ikeda, for HAL QCD Collaboration, in these proceedings.
 27. M. Lüscher, Nucl. Phys. B **354**, 531 (1991).
 28. S. Aoki, *et al.* [CP-PACS Collab.], Phys. Rev. D **71**, 094504 (2005).
 29. R. Tamagaki and W. Watari, Prog. Theor. Phys. Suppl. **39**, 23 (1967).
 30. J.J.de Swart, *et al.*, Springer Tracts in Modern Physics **60**, 138 (1971).
 31. S. Aoki *et al.* [PACS-CS Collaboration], Phys.Rev.D79, 034503 (2009), arXiv:0807.1661 [hep-lat].
 32. T. Yamanishi, Phys. Rev. D **76**, 014006 (2007) [arXiv:0705.4340 [hep-ph]].
 33. Reviewed in R. Machleidt and I. Slaus, J. Phys. G **27**, R69 (2001) [arXiv:nucl-th/0101056].